

A test of the frozen-flux approximation using a new geodynamo model

BY PAUL H. ROBERTS¹ AND GARY A. GLATZMAIER²

¹*Institute of Geophysics and Planetary Physics, University of California, Los Angeles, CA 90095, USA*

²*Earth Sciences Department, University of California, Santa Cruz, CA 95064, USA*

The physics underlying the frozen-flux approximation is reviewed. Recent high-resolution geodynamo simulations, described here for the first time, afford opportunities of testing the approximation, and the results from a very simple test are reported. This consists in evaluating the unsigned flux of magnetic field from the core at three successive epochs separated by about 150 years, and in showing that this changes by only *ca.* 3% in the intervals between the epochs. Because of the smallness of this change, which is created by the electromagnetic diffusion excluded in the frozen-flux approximation but present in the simulations, we argue that the approximation is useful in analogous analyses of the geomagnetic field over similar time-scales.

Keywords: geodynamo; computer simulations; frozen flux

1. Background to the approximation

The magnetic field, \mathbf{B} , in a body of conducting fluid such as the Earth's core is governed by the induction equation

$$\frac{\partial \mathbf{B}}{\partial t} = \nabla \times [\mathbf{v} \times \mathbf{B} - \eta \nabla \times \mathbf{B}], \quad (1.1)$$

and by

$$\nabla \cdot \mathbf{B} = 0. \quad (1.2)$$

Here \mathbf{v} is the velocity of the fluid and η is its magnetic diffusivity. Equation (1.2) is an initial condition; if it holds at time $t = 0$, it holds for all t according to (1.1).

Let us introduce a characteristic length-scale, \mathcal{L} , for \mathbf{B} and a characteristic flow speed, \mathcal{V} . Dimensionless analysis of (1.1) shows that \mathbf{B} evolves on two time-scales, the *advection time-scale*, τ_v , and the *time-scale*, τ_η :

$$\tau_v = \mathcal{L}/\mathcal{V}, \quad \tau_\eta = \mathcal{L}^2/\eta. \quad (1.3)$$

The ratio of these time-scales is the *magnetic Reynolds number*,

$$R = \tau_\eta/\tau_v = \mathcal{V}\mathcal{L}/\eta. \quad (1.4)$$

In order of magnitude this is the ratio of the second term in (1.1) to the third and, if

$$R \gg 1, \quad (1.5)$$

we are encouraged to omit the third term, giving the induction equation for a perfectly conducting fluid ($\eta = 0$):

$$\frac{\partial \mathbf{B}}{\partial t} = \nabla \times (\mathbf{v} \times \mathbf{B}). \quad (1.6)$$

Alfvén's frozen-flux theorem follows from (1.6): 'in a perfectly conducting fluid, magnetic flux tubes are material volumes', i.e. they move with the fluid as though frozen to it.

In applying these results to the geomagnetic field, we shall suppose that \mathbf{B} at a given point \mathbf{x} in the core varies rapidly, on the time-scale τ_v . By (1.1), the relative motion between material volumes and flux tubes is of order η/\mathcal{L} , which is small compared with \mathcal{V} by (1.5). The variation of \mathbf{B} at \mathbf{x} may therefore be visualized through Alfvén's theorem as the rearrangement of pre-existing magnetic flux by the fluid velocity \mathbf{v} . But, if we move with a small element of fluid volume δV as it is advected by the flow, we would find according to (1.1) that the flux threading δV changes slowly, on the time-scale $\tau_\eta \gg \tau_v$. If, then, we follow δV over a 'time-scale of observation', τ_O , that is of order τ_η or greater, we would find that the change in the threading flux would be so substantial as to make the frozen-flux approximation (1.6) valueless. In short, inequality (1.5) is an insufficient justification for replacing (1.1) by (1.6). Necessary conditions for frozen flux to be applicable are

$$\tau_v \ll \tau_\eta, \quad \tau_O \ll \tau_\eta. \quad (1.7)$$

When both these hold, Alfvén's theorem is useful both analytically and as a means of visualizing induction processes in the core.

2. Applicability of the approximation to the Earth's core

The period of time over which data of sufficient quality exist to test (1.6), and to make use of (1.6) if they survive the test, is not even as great as 100 years, though we shall take $\tau_O = 100$ yr. The traditional way of estimating \mathcal{V} for the core is through the westward drift of the field. This suggests that $\mathcal{V} = 5 \times 10^{-4} \text{ m s}^{-1}$ for features of scale $\mathcal{L} \approx 10^3 \text{ km}$, so that $\tau_v \approx 65$ yr, which is of the same order as the eddy turnover time in the Glatzmaier–Roberts geodynamo simulations (see Glatzmaier & Roberts 1996*b*, 1997). Taking $\eta = 2 \text{ m}^2 \text{ s}^{-1}$ (see, for example, Braginsky & Roberts 1995, Appendix E), we find that $R \approx 250$ and $\tau_\eta \approx 1.6 \times 10^4$ yr. It appears that both inequalities (1.7) are obeyed.

Because of its low kinematic viscosity, ν , the core is certainly in turbulent motion, with kinetic and magnetic energies spread over many scales \mathcal{L} . The use of the single scale above is clearly somewhat simplistic. Considered as a function of eddy size, the magnetic Reynolds number R should ultimately decrease with \mathcal{L} so that (1.5) is violated for all sufficiently small \mathcal{L} . Let us estimate very approximately the scale \mathcal{L}_c for which $R(\mathcal{L}_c) = 1$; roughly speaking, (1.6) is reasonable for $\mathcal{L} > \mathcal{L}_c$ and is unreasonable for $\mathcal{L} < \mathcal{L}_c$. The energy spectrum of the core is unknown, but let us suppose (as suggested by the computer simulations to be described in §3) that the kinetic energy K_ℓ in wavenumber ℓ is approximately proportional to $\ell^{-2.4}$. (Here ℓ refers to the spherical harmonic order in the decomposition of the total energy, poloidal and toroidal; see also (2.2).) This suggests that $\mathcal{V} \propto \mathcal{L}^{1.2}$ for eddies of scale \mathcal{L} , and that $R \propto \mathcal{L}^{2.2}$ for these eddies. If $R = 250$ for $\mathcal{L} \approx 10^3 \text{ km}$ (see above), then

$R = 1$ for $\mathcal{L}_c \approx 80$ km. This is comparable with the smallest scale, $\ell = L$, of \mathbf{B} that can be resolved on the core surface; $L \approx 12$ – 13 (see below). For $\mathcal{L}_c \approx 80$ km, we have $\tau_\eta = \mathcal{L}_c^2/\eta \approx 100$ yr. We conclude that both of the inequalities (1.7) are marginally satisfied for $\ell = L$ and $\tau_O \approx 100$ yr, and are increasingly well obeyed as ℓ decreases from L . If this is true then, as suggested by Roberts & Scott (1965), (1.6) should be a good approximation to (1.1) for the accessible length- and time-scales.

The Roberts–Scott idea encountered immediate difficulties. First, \mathbf{B} and $\partial\mathbf{B}/\partial t$ are known at the Earth’s surface, $r = a$, but (1.6) at best applies at S , the core surface, $r = c$. In between lies the mantle, and it is necessary to *extrapolate* \mathbf{B} through this. Since the electromagnetic time constant of the mantle, τ_η^M , is much smaller than τ_v (see, for example, Gubbins & Roberts 1987, § 3.3), $R^M \equiv \tau_\eta^M/\tau_v \ll 1$. This means that to a good approximation the mantle is an electrical insulator and, if there are no other sources in the mantle, \mathbf{B} is a potential field, $\hat{\mathbf{B}}$, not only on and above the Earth’s surface but also within the mantle:

$$\hat{\mathbf{B}} = -\nabla V, \quad \text{for } r > c, \quad (2.1)$$

where $\nabla^2 V = 0$ and where the usual expansion in exterior spherical harmonics applies:

$$V = a \sum_{\ell=1}^{\infty} \sum_{m=0}^{\ell} [g_\ell^m(t) \cos m\phi + h_\ell^m(t) \sin m\phi] (a/r)^{\ell+1} P_\ell^m(\theta). \quad (2.2)$$

Here (r, θ, ϕ) are geocentric spherical coordinates, with $\theta = 0$ as the north polar axis, P_ℓ^m are the Schmidt normalized Legendre functions and g_ℓ^m and h_ℓ^m are the Gauss coefficients.

In principle, we can evaluate $\hat{\mathbf{B}}$ at the base of the mantle by carrying out the differentiations (2.1) and setting $r = c$. In practice, difficulties arise. First, the assumption that there are no other sources of \mathbf{B} between $r = a$ and $r = c$ is incorrect; there is significant permanent magnetism in the crust, which makes the sum (2.2) meaningless at $r = c$ if taken beyond a cut-off $\ell = L$ of order 12 to 13. Second, because of inaccuracies and poor spatial coverage in the data, errors in g_ℓ^m and h_ℓ^m inevitably arise; these increase with ℓ , and they produce errors in $\hat{\mathbf{B}}$ that are further enhanced, by a factor proportional to $(a/c)^\ell$ that increases with ℓ , during extrapolation to the core surface. Nevertheless, when the series (2.2) is terminated at a value $L \approx 12$, techniques have been developed through which $\hat{\mathbf{B}}$ can be obtained on S with some degree of confidence, as many studies (too numerous to reference here) attest.

A further difficulty concerns the no-slip conditions which, in the reference frame rotating with the mantle (the frame we shall now employ until § 3), are

$$\mathbf{r} \cdot \mathbf{v} = 0, \quad \text{on } S \quad (2.3)$$

$$\mathbf{r} \times \mathbf{v} = \mathbf{0}, \quad \text{on } S \quad (2.4)$$

We have here used the radius vector \mathbf{r} from the geocentre as the normal to S . If we applied (2.4) to (1.6), we would find that $\hat{\mathbf{B}}$ is time-independent in the mantle frame. To resolve this absurdity, we have to consider the magnetohydrodynamics (MHD) of the core. The (molecular) viscosity, ν , of the core is thought to be smaller by a factor of about 10^6 than the (molecular) magnetic diffusivity, η (see, for example, Braginsky & Roberts 1995; De Wijs *et al.* 1998). Plausibly, therefore, there is a thin

boundary layer on S of Ekman-layer type in which viscous forces are significant. In the ‘mainstream’ beneath the layer, the flow is inviscid to leading order, and can obey (2.3) but not (2.4). The boundary-layer flow matches to the mainstream at a level indistinguishable from $r = c$ that we shall call the ‘top of the core’; the boundary-layer flow also satisfies conditions (2.3) and (2.4) on S . In this process it creates a small violation of (2.3) at the top of the core through a pumping process of the type associated with Ekman layers (see, for example, Greenspan 1968). We shall ignore this, and shall apply (2.3) at the top of the core, where the flow is therefore horizontal; we denote it by \mathbf{v}_H and term it the ‘surficial velocity’. It is clear from (1.2) that, to a very good approximation, the normal component B_r of \mathbf{B} is continuous across the boundary layer and is therefore equal to \hat{B}_r on S .

The frozen-flux approximation has been used on numerous occasions in efforts to determine \mathbf{v}_H . Because B_r does not change across the boundary layer, it is attractive to work with the r -component of (1.6), which is

$$\frac{\partial \hat{B}_r}{\partial t} = \nabla_H \cdot (v_r \hat{\mathbf{B}}_H - \hat{B}_r \mathbf{v}_H). \quad (2.5)$$

Ignoring pumping by the boundary layer, we find from (2.5) that

$$\frac{\partial \hat{B}_r}{\partial t} + \nabla_H \cdot (\hat{B}_r \mathbf{v}_H) = 0, \quad (2.6)$$

which may also be written as

$$\frac{\partial \hat{B}_r}{\partial t} + \mathbf{v}_H \cdot \nabla_H \hat{B}_r = -\hat{B}_r \nabla_H \cdot \mathbf{v}_H. \quad (2.7)$$

The frozen-flux approximation is disappointing in that it is impossible to derive the surficial velocity in full (or perhaps at all) from the field. There are serious problems of non-existence and non-uniqueness that should be addressed. Concerning non-existence, we introduce (following Backus 1968) the *null flux curves*, i.e. the curves on S on which \hat{B}_r is zero. An area of S that is enclosed by a null flux curve and in which \hat{B}_r has everywhere the same sign is called a *null flux patch*. There is one principal null flux curve, the *magnetic equator*, and several subsidiary null flux curves. It is easily shown from (2.6) that, since \mathbf{v}_H is finite everywhere and in particular on the null flux curves,

$$\frac{d}{dt} \int_P \hat{B}_r \, dS = 0, \quad (2.8)$$

where the integral is taken over a null flux patch P and d/dt includes the time evolution of P . This result is no more than an example of Alfvén’s theorem applied to the cross-section, P , of a flux tube emerging from the core. If we take all the null flux curves together, we see from (2.8) that

$$\oint_S |\hat{B}_r| \, dS = \text{constant for all } t, \quad (2.9)$$

this integral of *unsigned flux*, $|\hat{B}_r|$, being taken over the entire core surface S . Of course, (2.9) does not imply that (2.8) holds for each individual null flux patch.

There are two reasons why no straightforward analysis of the geomagnetic data will confirm (2.8), where by ‘straightforward analysis’ we mean one that ignores the frozen-flux approximation. First, there are what we shall call errors of type 1: even if (2.8) were true, data analysis would not confirm it because of errors in, and the incompleteness of, available data and because of the difficulties inherent in extrapolating fields accurately from the Earth’s surface to the core surface. Second (the error of type 2), because of electromagnetic diffusion, (2.8) is not precisely true anyway. The basic tenet of Roberts & Scott (1965) was that error 1 is much more significant than error 2. If this is true, all claims that deviations from (2.8) have been discovered must be viewed with suspicion. Moreover, if error 2 is swamped by error 1, nothing is lost by eliminating error 2 totally through a non-straightforward data analysis in which (2.8) is imposed as a constraint.

The idea of adding constraints to geomagnetic analyses is, of course, nothing new. For example, analyses are often performed with the series (2.2) rather than the full representation that also includes the exterior harmonics; in other words, the analyses have been constrained *a priori* to exclude the exterior harmonics. The Roberts–Scott proposal was merely to add a new form of constraint. Such analyses have been performed by Constable *et al.* (1993) and O’Brien *et al.* (1997). Not only is nothing lost by such analyses, but also something is gained, namely the certainty that a finite \mathbf{v}_H exists. This \mathbf{v}_H is not unique. Roberts & Scott (1965) provided a simple example. If the surficial velocity is purely toroidal, $\nabla_H \cdot \mathbf{v}_H = 0$, and (2.7) reduces to

$$\frac{\partial \hat{B}_r}{\partial t} + \mathbf{v}_H \cdot \nabla_H \hat{B}_r = 0. \quad (2.10)$$

If \mathbf{v}_H is one solution to (2.10) for the assigned \hat{B}_r and $\partial \hat{B}_r / \partial t$, then $\mathbf{v}_H + \mathbf{r} \times \nabla_H f$ is another, where $f(\hat{B}_r)$ is any function that is constant on each constant- \hat{B}_r contour on S . A much more complete and satisfying discussion of non-existence and non-uniqueness was later provided by Backus (1968). Several proposals have been made to remove the non-uniqueness by supplementing the frozen-flux approximation with additional hypotheses, but we shall not review these.

The developments just described are all based on the idea that the frozen-flux approximation is an adequate way of describing the evolution of \mathbf{B} in the mainstream beneath the boundary layer, i.e. that not only ν but also η can be assumed to be zero at leading order. Since the geodynamo problem concerns countering magnetic diffusion by motional induction, how can it be right to use (1.6) instead of (1.1) in the mainstream? Recently Love (1999) has given two ingenious kinematic examples to show how (1.6) leads to \mathbf{v}_H quite different from the actual surficial velocity of the flow maintaining the dynamo. The first of these is steady, and therefore does not satisfy the requirement of §1 that \mathbf{B} evolves on the τ_v time-scale. The same seems to be true of Love’s (1999) second model, though both \mathbf{v} and \mathbf{B} are time dependent in that case. Since we have no ambitions in this paper to infer \mathbf{v}_H , we shall not enter into these controversial matters here.

Other doubts about the value of the frozen-flux approximation hinge on whether errors of type 2 are smaller than those of type 1. This is a delicate matter for, while error 2 must be greater for a small-scale patch than a large-scale patch because its electromagnetic time constant is smaller, error 1 is also greater because the patch is described by higher harmonics ℓ of the field, the errors in which are much larger, especially after extrapolation to S . In claiming that they have strong evidence that

new flux is emerging from the core into the mantle from a secular variation centre under and to the west of Africa, Bloxham & Gubbins (1986) are implying that error 2 can be detected despite error 1. If there is a strong subsurface toroidal field in the core, it is easy to imagine that a poloidal upwelling, in which $\nabla_{\text{H}} \cdot \mathbf{v}_{\text{H}} \neq 0$, will push toroidal field through S and into the mantle. Several models of such a process have been constructed (Coulomb 1954, 1955; Allan & Bullard 1958, 1966; Hide & Roberts 1961; Nagata & Rikitake 1961; Rikitake 1967; Bloxham 1986; Drew 1993). There is no doubt that such processes can and must occur in the Earth, but it is less clear how far they discredit the frozen-flux approximation. At the time the early papers just referenced were written, it appeared that they posed a serious threat to the frozen-flux approximation, but in recent simulations of the geodynamo the toroidal fields have been comparable with the poloidal fields, not much larger as had previously been expected (see, for example, Glatzmaier & Roberts 1996*b*, 1997). These geodynamo simulations also suggest that toroidal fields are relatively weak near the core–mantle boundary compared with those near the inner-core boundary. The creation of new poloidal flux in the mantle by upwellings in the core may therefore not be as rapid as had been thought.

A further concern centres on the effects of small-scale turbulence on the large-scale field and flow (belonging to $\ell \leq L$). The EMF $\mathbf{v} \times \mathbf{B}$ created by small-scale \mathbf{v} and \mathbf{B} has a part that alters the large-scale field. The way it does so defines the subject of *mean field electrodynamics* (see, for example, Krause & Rädler 1980). The large-scale EMF from the turbulence is parametrized as $\alpha\mathbf{B} - \beta\nabla \times \mathbf{B}$ (for example), where \mathbf{B} is now the large-scale field; $\alpha\mathbf{B}$ defines the so-called α -effect and β represents a turbulent enhancement of the molecular diffusivity η . Braginsky & Meytlis (1990) argue cogently that these terms are insignificant in the MHD of the Earth's core.

The situation is different for the turbulent transport of momentum. As we have seen, the molecular viscosity ν of the core is about 10^6 times smaller than η , and turbulence is required, and exists, to transport momentum. The Reynolds analogy provides an approximate way of parametrizing this process, through the introduction of a 'turbulent viscosity' ν^t of order η . Turbulent transport alters the structure of boundary layers, an effect that has been observed, for example, in ocean physics (see Hunkins 1966). Because $\nu^t \approx \eta$, the boundary layer on S may more closely resemble an Ekman–Hartmann layer (Gilman & Benton 1968) than the Ekman layer invoked earlier. If so, $\mathbf{r} \times \mathbf{B}$ will change significantly across the layer, so that $\mathbf{r} \times \mathbf{B}$ at the top of the core will differ from $\mathbf{r} \times \hat{\mathbf{B}}$ on S . The tangential components of (1.6) will then not be immediately useful in inferring \mathbf{v}_{H} . The boundary layer is thin, however, so that the validity of (2.6) is not affected.

Questions similar to these arise in numerical simulations, where the effect of the unresolved scales of \mathbf{v} and \mathbf{B} on the resolved scales may require parametrization. This matter will arise below, where we shall suppose (as above) that the molecular EMF need not be modified. We shall find it necessary, however, to increase ν even beyond $\nu^t \approx \eta$.

3. Application of the approximation to numerical simulations

The uncertainties introduced by the data errors and their incompleteness, combined with the difficulties of extrapolation to the core surface, make it hard to decide how seriously the frozen-flux approximation is violated in the Earth's core during the

time $\tau_O \approx 100$ yr over which it has been closely observed. Recently, however, there have been several numerical simulations of the geodynamo that have produced fields that have resembled the geomagnetic field both in structure and evolution (see, for example, Glatzmaier & Roberts 1996*b*, 1997). Since simulations directly provide \mathbf{B} on the core surface, they completely eliminate errors of type 1, and they do so in an Earth-like context. The idea of using such simulations to test the frozen-flux approximation is attractive and has been attempted by Glatzmaier & Roberts (1996*a*), with encouraging results. But these tests can be criticized because the simulations on which they are based required hyperdiffusion in order to secure numerical convergence, and hyperdiffusion of \mathbf{B} violates frozen flux. Recently, however, we have produced a very high-resolution geodynamo simulation without hyperdiffusion, which is quite suitable for testing frozen flux. Results from this model are presented here for the first time. We know *a priori* that type-2 errors must be present, so that (2.8) cannot be precisely true. The test of the frozen-flux hypothesis must therefore be modified. It becomes ‘how well is (2.8) obeyed’? We shall ask only ‘how well is the unsigned flux (2.9) from the core conserved’? Since (2.9) does not imply (2.8), this is a more limited objective.

We solve the MHD convection equations in the form proposed by Braginsky & Roberts (1995) and in a frame of reference in which the total angular momentum of Earth is zero. This means that the mantle and therefore the core–mantle boundary are in slow solid-body rotation, so although (2.4) is satisfied in the frame of the mantle, it is not in our frame of reference. This rotation, which is quite small (of order 3×10^{-4} deg yr $^{-1}$), has not been removed in the figures presented here. All diffusivities, with the exception of ν , are assumed to be $7 \text{ m}^2 \text{ s}^{-1}$. Because we have used $\eta = 7 \text{ m}^2 \text{ s}^{-1}$ rather than the geophysically more realistic $2 \text{ m}^2 \text{ s}^{-1}$, we shall, in what follows, reinterpret time-scales by multiplying them by the ratio, 3.5, of these two values of η , so that all velocities will be reduced by the same factor. For example, the scaled rotation of the core boundary is of order 10^{-4} deg yr $^{-1}$. Nevertheless, we recognize that such a rescaling of the MHD equations strictly requires the rotation of Earth to be reduced by the same factor, and this has not been done. Typical core velocities \mathcal{V} are of order $3 \times 10^{-4} \text{ m s}^{-1}$, and the overturning time of large-scale core eddies is *ca.* 200 yr. These values are consistent with those used in § 2 to motivate the frozen-flux approximation. As in our earlier simulations, it is necessary to use a viscosity even larger than η ; after scaling it is $1500 \text{ m}^2 \text{ s}^{-1}$.

Glatzmaier & Roberts (1996*b*) used the spectral transform technique in their numerical work. In their 1996 simulation, all harmonics were included in the expansion of \mathbf{v} and \mathbf{B} up to $\ell = m = 21$. In the present highly resolved model, a trapezoidal truncation is employed: 120 Fourier modes ($0 \leq m \leq 119$) in longitude are included and, for each m , all values of ℓ are present from m to $120 + m$. The largest value of ℓ appearing anywhere is therefore $\ell = 239$, which occurs for $m = 119$. The Chebychev expansion in r was up to 48 in the fluid core and up to 32 in the solid core. The integration was initiated from a case of low resolution.

The greater spatial resolution of the new model (60 times as many spherical harmonics) required a small numerical time-step (7 days) because of the demands of the magnetic Courant condition. The computational expense is very great, and so far the model has been integrated for only about 1400 years of simulated time. This was far enough for all the transients connected with the initialization of the computation to have disappeared. This is confirmed by figure 1, which shows the magnetic and

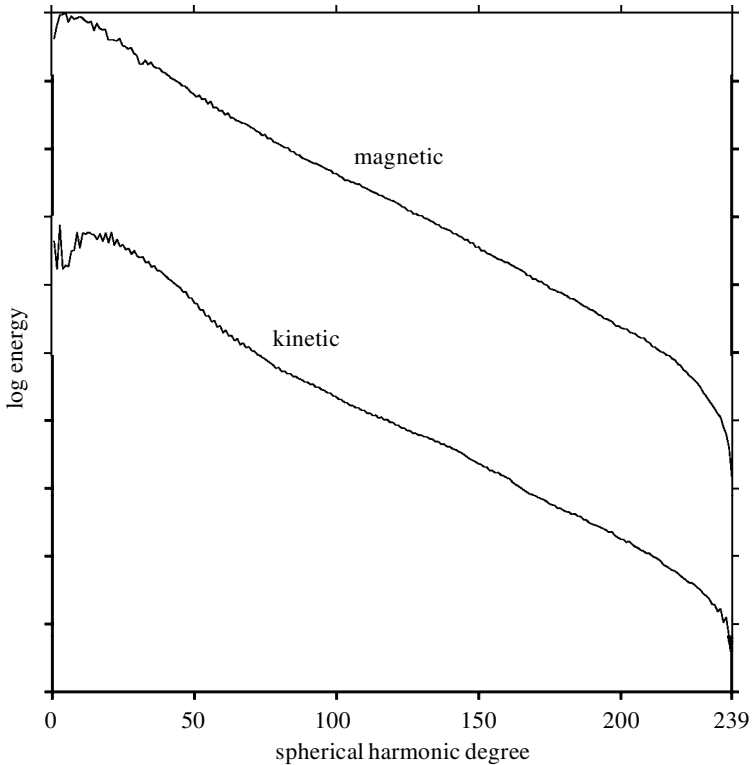


Figure 1. Power spectra of the magnetic energy (upper curve) and kinetic energy (lower curve) integrated throughout the fluid core at epoch 2, as a function of ℓ for $0 < \ell < 240$. The spectra are given logarithmically, in arbitrary units which cover 10 decades; the kinetic energy is consistently about a thousand times less than the magnetic energy. The representation of the field and flow used to obtain these results employed a trapezoidal truncation; 120 Fourier modes ($0 \leq m \leq 119$) in longitude are included and, for each m , all values of ℓ are present from m to $120 + m$. The largest value of ℓ appearing anywhere is therefore $\ell = 239$, which occurs for $m = 119$.

kinetic energies (relative to the rotating frame of reference) integrated throughout the fluid core as a function of the spherical harmonic degree ℓ . It was not, however, long enough for the system to have evolved far from its initial state, which was quite soon after a magnetic dipole reversal had taken place. This may be seen both from the comparatively small energy in the $\ell = 1$ field (figure 1), and later from the untypically large deviation of the geomagnetic equator from the geographical equator in one large band of longitude. The fact that the field is transitional in no way detracts from its usefulness in testing the frozen-flux approximation, quite the reverse in fact. Since the unsigned flux changes more rapidly during transition than between reversals, these fields provide a particularly stringent test of the approximation. Figure 1 also demonstrates that the solution has converged satisfactorily, without hyperdiffusion. The magnetic energy is about three orders of magnitude greater than the kinetic energy, and has a broad peak between harmonic degrees $\ell = 5$ – 15 .

We focus on three snapshots of the solution, each separated from its neighbour by approximately 150 years of simulated time ($\tau_{\text{O}} = 150 \text{ yr}$). We shall refer to these

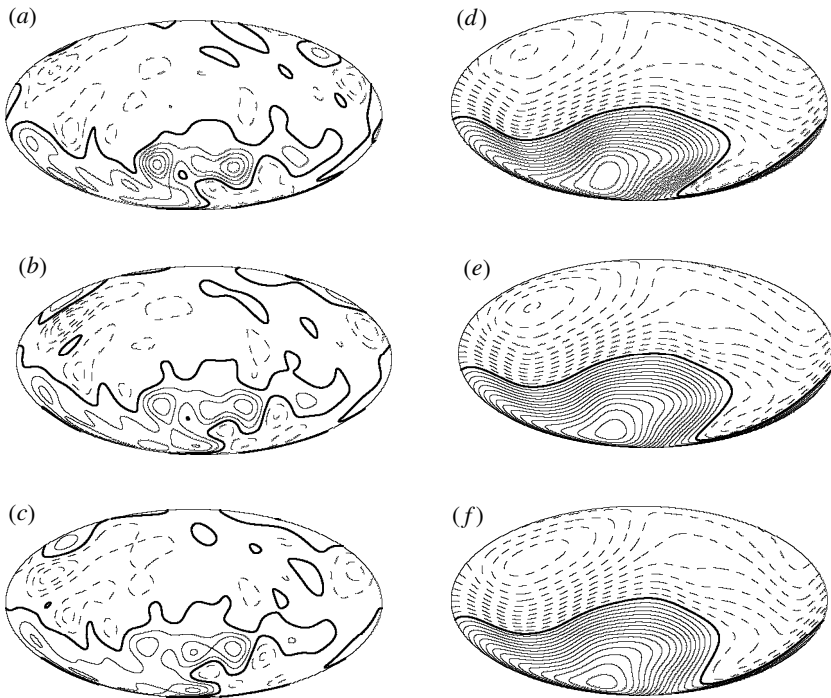


Figure 2. Contours of equal \hat{B}_r on the core surface (a)–(c) and on the Earth’s surface (d)–(f). (a), (d) epoch 1; (b), (e) epoch 2; (c), (f) epoch 3. The truncation level L is 12. The bold full curves are magnetic equators, $\hat{B}_r = 0$. On the continuous curves $\hat{B}_r > 0$; on the dashed curves $\hat{B}_r < 0$. The contour interval is 7 G for the core surface and 0.1 G for the Earth’s surface.

as ‘epoch 1’, ‘epoch 2’ and ‘epoch 3’. (Because of the infrequency of data dumps, separations at the shorter $\tau_0 \approx 100$ yr intervals were not available.) Figure 2 shows, in equal-area projections, contours of constant \hat{B}_r on the Earth’s surface and on the core surface for each epoch. Figure 2 is drawn for $L = 12$, and figure 3 presents the same plots for $L = 72$. It is striking how much of the small-scale structure, associated with large ℓ , is lost at the Earth’s surface through the geometric attenuation factor $(c/a)^{\ell+2}$ (see (2.2)). Using epoch 3 as an illustration, figure 4 shows how structure develops on the core surface as L is increased. The changes from one panel to the next tend to diminish as L increases; the fields at $L = 60$ and $L = 72$ are very similar. This is also consistent with the results shown in table 1, where the maximum and minimum \hat{B}_r are given for the same six values of L as figure 4.

These figures underscore the limitations imposed by geometry in extrapolating \hat{B}_r downwards; it is quite difficult to distinguish the plots of \hat{B}_r at the core surface for the $L = 12$ truncation from those for the $L = 72$ truncation at the same epoch, even though the fields at the core surface are very different. (Indeed, the same may be said at the $L = 12$ and $L = 24$ levels.) Certainly, the same must be true for the Earth. Estimates of \hat{B}_r at the Earth’s core–mantle boundary using $L = 12$ are necessarily of large scale, but these highly filtered results do not imply that the actual core–mantle boundary field is dominantly of large scale. Likewise, the surficial flow, \mathbf{v}_H , based on these highly filtered core–mantle boundary-field structures will also tend to be of

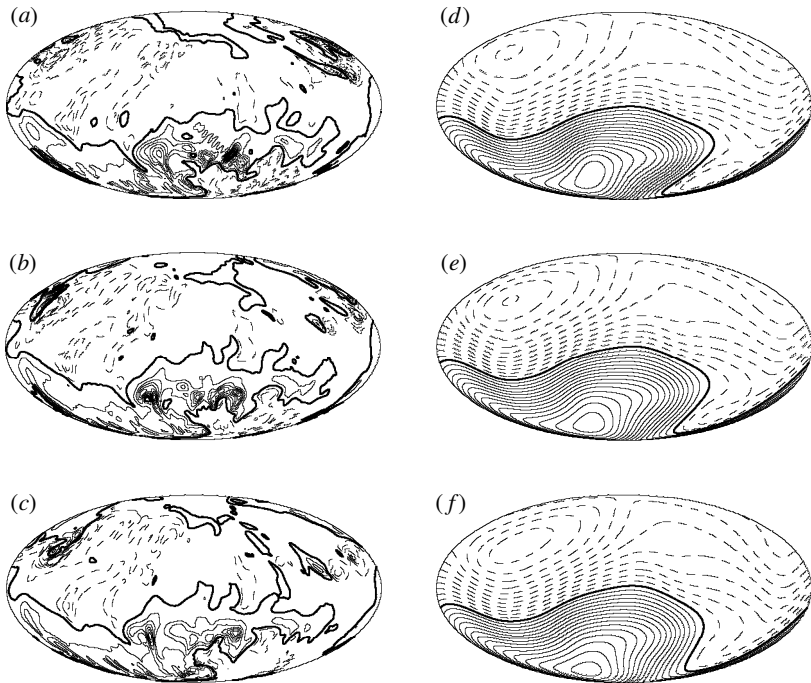


Figure 3. Contours of equal \hat{B}_r on the core surface (a)–(c) and on the Earth’s surface (d)–(f). (a), (d) epoch 1; (b), (e) epoch 2; (c), (f) epoch 3. The truncation level L is 72. The bold full curves are magnetic equators, $\hat{B}_r = 0$. On the continuous curves $\hat{B}_r > 0$; on the dashed curves $\hat{B}_r < 0$. The contour interval is 7 G for the core surface and 0.1 G for the Earth’s surface.

large scale but, if \hat{B}_r at the core–mantle boundary were accurately known to $\ell = 239$ as in the simulation, the surficial flow would be dominated by small scales.

According to the frozen flux approximation, field topology cannot change on the core surface. However, when we compare panels figure 2a–c at the $L = 12$ truncation and figure 3a–c at $L = 72$ we see this is only true for the large null flux patches. This is only to be expected since $L = 72$ corresponds to \mathcal{L} much smaller than 80 km, and τ_η for $L = 72$ is much less than 100 years. Another interesting feature of the high- L plots is the presence of small regions of very high flux, ‘core spots’, somewhat analogous to the sunspots observed on the solar surface.

Turning next to the question of the conservation (2.9) of unsigned flux, we divided the core surface S into 180×180 ‘rectangles’ of equal surface area, and summed \hat{B}_r and $|\hat{B}_r|$ from each, to provide estimates of

$$F = \oint_S \hat{B}_r \, dS, \quad (3.1)$$

$$U = \oint_S |\hat{B}_r| \, dS. \quad (3.2)$$

The flux integral, F , should be zero by (1.2), and its numerical value gives some feeling for the accuracy to which the unsigned flux, U , has been obtained. We found that $|F| \approx 10^{-4}U$. A further test was carried out in which S was divided into 360×360 rectangles, and the results did not differ to the accuracy shown in table 2,

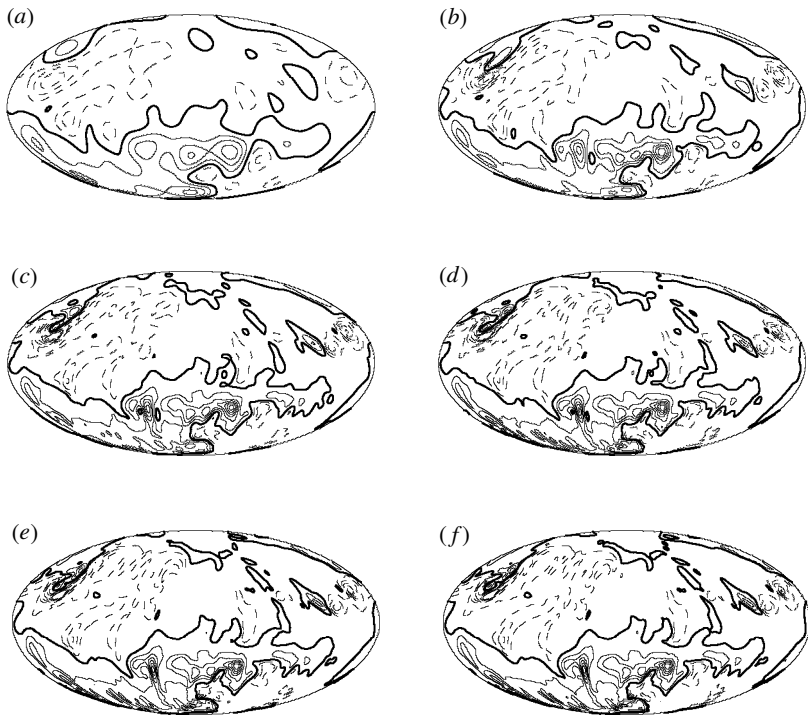


Figure 4. Contours of equal \hat{B}_r on the core surface for epoch 3 at different truncation levels: (a) $L = 12$; (b) $L = 24$; (c) $L = 36$; (d) $L = 48$; (e) $L = 60$; (f) $L = 72$. The bold full curve is the magnetic equator, $\hat{B}_r = 0$. On the continuous curves $\hat{B}_r > 0$; on the dashed curves $\hat{B}_r < 0$. The contour interval is 7 G.

Table 1. Maxima and minima of \hat{B}_r on the core surface as functions of the truncation level, L , for epoch 3

(Unit of $\hat{B}_r = 1$ G.)

L	12	24	36	48	60	72
$\hat{B}_{r,\max}$	26	42	46	49	49	49
$-\hat{B}_{r,\min}$	26	44	64	70	76	76

where U is given as a function of the cut-off L for the three epochs. Beyond $L = 36$, the unsigned flux does not change to the accuracy shown. The averages of $|\hat{B}_r|$ over the core surface for the three epochs are, respectively, 6.4, 6.2 and 5.9 G.

It may be seen from table 2 that, at the geomagnetic ($L = 12$) truncation, the change in U over 150 years is only *ca.* 3%, or *ca.* 2% per century, corresponding to field changes on the core surface of order 0.1 G. In the corresponding geophysical context, the question to be answered is whether this type-2 error (to use our earlier terminology) is large or small compared with the type-1 errors arising from inaccuracies in, and the incompleteness of, the available data, and the difficulties of extrapolation to the core surface. The error of extrapolation may be roughly assessed from the simulation by asking how much of the U obtained at the $L = 36$ truncation has been omitted in the $L = 12$ truncation. Comparing the second and fourth columns of

Table 2. Evolution of the unsigned flux, U , from the Earth's core for three truncation levels L (Unit of flux is 10^{18} G cm².)

epoch	$L = 12$	$L = 24$	$L = 36$
1	9.3	9.6	9.7
2	9.0	9.4	9.5
3	8.7	9.0	9.0

table 2 it appears that this is at least as great as the variations within column 1 (the type-2 error). Since this is only one part of the type-1 error, we conclude that the frozen-flux approximation provides a way of modelling the geomagnetic field that is acceptable in view of the greater type-1 errors inherent in modelling the geomagnetic field on the core surface. This also supports the approach of Constable *et al.* (1993) and O'Brien *et al.* (1997) to geomagnetic field analysis.

This work was supported by the National Science Foundation under grants EAR97-25627 and EAR99-02969 and by the SDSC and NCSA Supercomputing Centers. It was also supported by the Institute of Geophysics and Planetary Physics, the University of California Partnership Initiatives Program and the Advanced Computing Laboratory, all at the Los Alamos National Laboratory. We are grateful to Maureen Roberts for preparing the figures, and the referees for their criticisms.

References

- Allan, D. E. & Bullard, E. C. 1958 Distortion of a toroidal field by convection. *Rev. Mod. Phys.* **30**, 1087–1088.
- Allan, D. E. & Bullard, E. C. 1966 The secular variation of the Earth's magnetic field. *Proc. Camb. Phil. Soc.* **62**, 783–809.
- Backus, G. E. 1968 Kinematics of geomagnetic secular variation in a perfectly conducting core. *Phil. Trans. R. Soc. Lond. A* **263**, 239–266.
- Bloxham, J. 1986 The expulsion of magnetic flux from Earth's core. *Geophys. Jl R. Astr. Soc.* **87**, 669–678.
- Bloxham, J. & Gubbins, D. 1986 Geomagnetic field analysis. IV. Testing the frozen-flux hypothesis. *Geophys. Jl R. Astr. Soc.* **84**, 139–152.
- Braginsky, S. I. & Meytlis, V. P. 1990 Local turbulence in the Earth's core. *Geophys. Astrophys. Fluid Dynam.* **55**, 71–87.
- Braginsky, S. I. & Roberts, P. H. 1995 Equations governing convection in Earth's core and the geodynamo. *Geophys. Astrophys. Fluid Dynam.* **79**, 1–97.
- Constable, C. G., Parker, R. L. & Stark, P. B. 1993 Geomagnetic field models incorporating frozen flux constraints. *Geophys. Jl Int.* **113**, 419–433.
- Coulomb, J. 1954 Contribution à la théorie de la variation séculaire du magnétisme terrestre. *Rev. Fac. Sci. Univ. Istanbul C* **19**, 200–213.
- Coulomb, J. 1955 Variation séculaire par convergence à la surface du noyau. *Ann. Geophys.* **11**, 80–82.
- De Wijs G. A., Kresse, G., Vočadlo, L., Dobson, D., Alføe, D., Gillan, M. J. & Price, G. D. 1998 The viscosity of liquid iron at the physical conditions of the Earth's core. *Nature* **392**, 805–807.
- Drew, S. J. 1993 Magnetic field expulsion into a conducting mantle. *Geophys. Jl Int.* **115**, 303–312.

- Gilman, P. A. & Benton, E. R. 1968 Influence of an axial magnetic field on the steady linear Ekman boundary layer. *Phys. Fluids* **11**, 2397–2401.
- Glatzmaier, G. A. & Roberts, P. H. 1996a On the magnetic sounding of planetary interiors. *Phys. Earth Planet. Interiors* **98**, 207–220.
- Glatzmaier, G. A. & Roberts, P. H. 1996b An anelastic evolutionary geodynamo simulation driven by compositional and thermal convection. *Physica D* **97**, 81–94.
- Glatzmaier, G. A. & Roberts, P. H. 1997 Simulating the geodynamo. *Contemp. Phys.* **38**, 269–288.
- Greenspan, H. P. 1968 *The theory of rotating fluids*. Cambridge University Press.
- Gubbins, D. & Roberts, P. H. 1987 Magnetohydrodynamics of the Earth's core. In *Geomagnetism* (ed. J. A. Jacobs), vol. 2. Academic.
- Hide, R. & Roberts, P. H. 1961 The origin of the main geomagnetic field. *Phys. Chem. Earth* **4**, 25–98.
- Hunkins, K. 1966 Ekman drift currents in the Arctic Ocean. *Deep-Sea Res.* **13**, 607–620.
- Krause, F. & Rädler, K.-H. 1980 *Mean-field magnetohydrodynamics and dynamo theory*. Oxford: Pergamon.
- Love, J. J. 1999 A critique of the frozen-flux inverse modelling of a nearly steady geodynamo. *Geophys. J. Int.* **138**, 353–365.
- Nagata, T. & Rikitake, T. 1961 Geomagnetic secular variation and poloidal magnetic fields produced by convectonal motion in the Earth's core. *J. Geomagn. Geoelectr.* **13**, 42–53.
- O'Brien, M. S., Constable, C. G. & Parker, R. L. 1997 Frozen-flux modeling for epochs 1915 and 1980. *Geophys. J. Int.* **128**, 434–450.
- Rikitake, T. 1967 Non-dipole field and fluid motion in the Earth's core *J. Geomagn. Geoelectr.* **19**, 129–142.
- Roberts, P. H. & Scott, S. 1965 On analysis of the secular variation. 1. A hydromagnetic constraint: theory. *J. Geomagn. Geoelectr.* **17**, 137–151.